EARLY RESULTS FROM THE FIRST RADARSAT-1 ANTARCTIC MAPPING MISSION

Proceedings Papers Submitted to

International Geoscience and Remote Sensing Society Meeting
Seattle, Washington
July, 1998

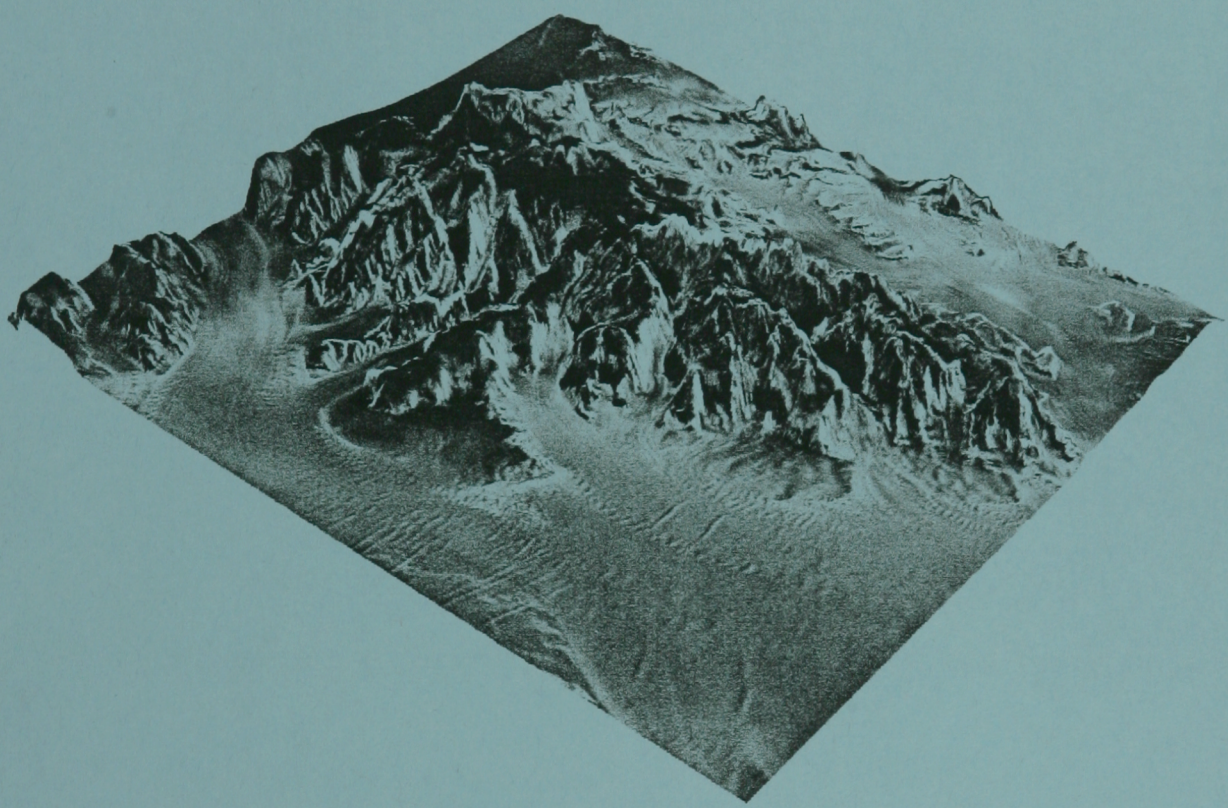

BYRD POLAR RESEARCH CENTER
THE OHIO STATE UNIVERSITY

BPRC Technical Report 98-02

BYRD POLAR RESEARCH CENTER
THE OHIO STATE UNIVERSITY
COLUMBUS, OHIO 43210-1002

EARLY RESULTS FROM THE FIRST

RADARSAT-1 ANTARCTIC MAPPING MISSION

Proceedings Papers Submitted to

International Geoscience and Remote Sensing Society Meeting
Seattle, Washington
July, 1998

edited by

Kenneth C. Jezek
Byrd Polar Research Center
The Ohio State University
Columbus, OH

April 8, 1998

Compiled in 1998 by the

BYRD POLAR RESEARCH CENTER

This report may be cited as:

Jezek, Kenneth C. 1998. *Early Results From the First Radarsat-1 Antarctic Mapping Mission.* BPRC Technical Report No. 98-02, Byrd Polar Research Center, The Ohio State University, Columbus, Ohio, 22 pages.

The Byrd Polar Research Center Report Series is edited by Lynn Tipton-Everett.

Copies of this and other publications of the Byrd Polar Research Center are available from:

Publication Distribution Program
Byrd Polar Research Center
The Ohio State University
1090 Carmack Road
Columbus, Ohio 43210-1002
Telephone: 614-292-6715

Preface

The Radarsat-1 Antarctic Mapping Mission (RAMP) is a collaborative effort between the Canadian Space Agency and the US National Aeronautics and Space Administration. The major participants in RAMP are The Ohio State University, The Alaska SAR Facility, The Jet Propulsion Laboratory and Vexcel Corporation. The goal of the collaboration is to create the first, complete high-resolution radar mosaic of all of Antarctica for studies of Antarctic glaciology, geology, meteorology and coastal processes.

The following papers describe early scientific results from the first RAMP Antarctic Imaging Campaign (AIC) which occurred from September to October of 1997. The papers have been accepted for presentation at the July 1998 meeting of the International Geoscience and Remote Sensing Society meeting, Seattle, WA. Also included is a paper which utilized ERS SAR data to study the geology of the Antarctic Peninsula. Techniques developed in that project will be applied to geologic studies of all of Antarctica.

This collection begins with an overview paper summarizing the complex execution of the first AIC in the context of pre-mission objectives. This is followed by a paper describing the techniques which will be used to process the data into a final, seamless mosaic. Several papers illustrate the extraordinary variety of terrain that Radarsat imaged as it flew over the Antarctic Continent during the AIC. Those papers go on to discuss newly discovered ice streams, the geologic significance of complex lineaments across all of Antarctica, and the potential for using RAMP data with other historical data sets for studies of ice flow variations. Initial interferometric results are also presented which strongly suggest that the great volume of repeat pass data collected during the AIC will be very useful for glaciologic studies.

The extraordinary success of RAMP in achieving pre-mission objectives is a result of the exceptional cooperation and commitment of many individuals in Canada and the US. This level of commitment will continue through the final map production to guarantee that the full scientific value of this rich data set is available to the international science community.

Kenneth C. Jezek
RAMP Principal Investigator

Snapshots of Antarctica from Radarsat-1

K. C. Jezek[1], F. Carsey[2], J. Crawford[2], J. Curlander[3], B. Holt[2], V. Kaupp[4], K Lord[5], N. Labelle-Hammer[4], A. Mahmood[5], P. Ondrus[6], C. Wales[4]

1. Byrd Polar Research Center, The Ohio State University, Columbus OH 43210
2. Jet Propulsion Laboratory, 4800 Oak Grove Drive, Pasadena CA
3. Vexcel Corporation, Boulder Colorado
4. Alaska SAR Facility, University of Alaska, Fairbanks, AK
5. Canadian Space Agency, St. Hubert, Canada
6. Goddard Space Flight Center, Greenbelt, Maryland

INTRODUCTION

Carried aloft by a NASA rocket launched from Vandenburg Air Force Base on November 4, 1995, the Canadian Radarsat-1 is equipped with a C-band Synthetic Aperture Radar (SAR) capable of acquiring high resolution (25 m) images of Earth's surface day or night and under all weather conditions. Along with the attributes familiar to researchers working with SAR data from the European Space Agency's Earth Remote Sensing Satellite and the Japanese Earth Resources Satellite, Radarsat-1 has enhanced flexibility to collect data using a variety of swath widths, incidence angles and resolutions. Most importantly, for scientists interested in Antarctica, Radarsat-1 can be maneuvered in orbit to rotate the normally right-looking SAR to a left-looking mode. This 'Antarctic Mode' provides for the first time a nearly instantaneous, high-resolution view of the entirety of Antarctica on each of two proposed mappings separated by 2 years. The first, Antarctic Imaging Campaign began on September 9, 1997 and was successfully concluded on October 20, 1997.

ANTARCTIC IMAGING CAMPAIGN

The first Antarctic Imaging Campaign (AIC) represents the culmination of many years of planning by Canada and the United States to complete the synthetic aperture radar (SAR) mapping of Antarctica [1,2,3]. The AIC was made possible by the unique capabilities of Radarsat-1 including an electronically steerable antenna array that provided a range of selectable beam pointing angles. This capability was essential for maximizing the range of the acquisition swaths from the satellite's nadir track. The satellite also has the capability to maneuver in orbit enabling it to change the look direction of the SAR. This capability permitted acquisitions to the Earth's South Pole and represents a technical ability afforded by no other civilian radar.

The AIC relied on real-time, transcontinental coordination of the ground-station network, which also included acquisitions in Antarctica during the early part of the mission. Operational and scientific information were transmitted between the various stations and to mission operations at the Canadian Space Agency in Montreal. The information was key to resolving the limited number of acquisition anomalies that occurred during the mission and quickly grasping scientific opportunities presented as the mission unfolded.

Finally the entire Radarsat-1 Antarctic Mapping Mission Project relied on the participation of many organizations in Canada and the United States and on scientific contributions from the international Antarctic Research Community. The major participants in RAMP are identified in fig. 1.

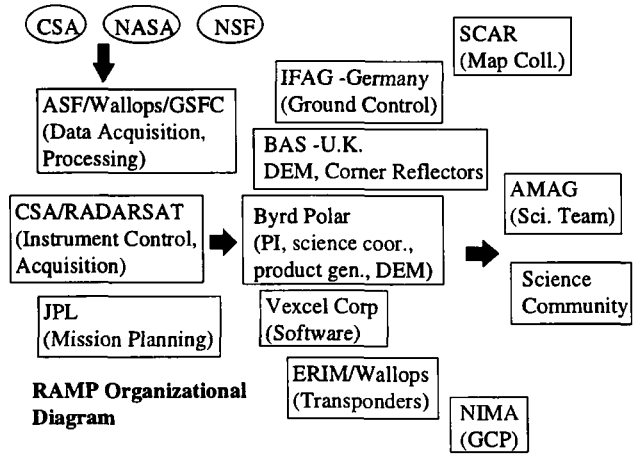

Figure 1. Organizational diagram for RAMP. Left most units are responsible for AIC acquisitions. Middle units are responsible for mosaic development. Right most units are responsible for quality control and science utilization.

AIC CHRONOLOGY

Starting on September 9, the Canadian spacecraft, Radarsat-1, temporarily ceased normal (right-looking) mode operations and began preparations for the Antarctic imaging maneuver. On September 10, the CSA spacecraft operations team in St. Hubert rotated the satellite 180 degrees from its normally right looking mode to a left looking mode. The procedure included a pitch down to –85 degrees, a yaw around to –180 degrees an a pitch up to 0 degrees to straight and level flight.

The spacecraft was gradually readied for operations on September 11. This included rotation of the solar panels and enabling payload heaters. The first Antarctic Mode image was acquired on September 12 and the first standard beam image of the Antarctic, stored on the on-board recorder, followed soon after. The first radar image of the Earth's South Pole was acquired on September 15 (fig. 2) and began the final stage of the radar mapping of Earth.

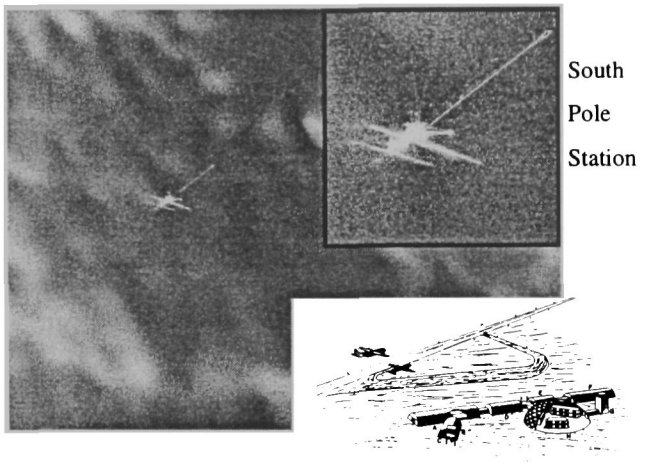

Figure 2. First synthetic aperture radar image of Earth's South Pole showing the location of Amundsen-Scott South Pole Station. South Pole Station is located in the radar clutter in the center of the inset. The central line running roughly from left to right is the current runway. The line segment to the lower left is the signature of the runway abandoned in 1974 and now buried. Old South Pole Station, also buried, is located between the two runways. The long line running to the upper right is a road to an abandoned science site. The road is about 8 km long.

The satellite was cleared for payload operations on September 16 and downlink and processing at the Alaska SAR Facility were confirmed by September 17. Because each of the payload milestones were crossed on schedule and because of the power, thermal and attitude stability of the spacecraft, CSA began to acquire images of the Antarctic on September 19 in support of RAMP. Routine tape recorder downlinking activities began at Gatineau, Prince Albert and the Alaska SAR Facility. Real time downlinks were also recorded at the McMurdo Ground Station.

The pre-AIC acquisitions (fig. 3) were culled from the nominal plan by relying on the 100 orbit near repeat cycle of the satellite. Acquisitions only imagable in South looking mode and located around the South Pole were identified as the highest priority. The data constituted an important contingency against anomalies encountered later in the mission.

The nominal acquisition plan (fig. 4) started on schedule shortly after noon EST on September 26. The plan was developed by the Jet Propulsion Laboratory and designed to obtain complete mapping coverage within 18 days. The nominal plan proceeded nearly flawlessly through completion on October 14.

Figure 3. Pre-AIC acquisitions

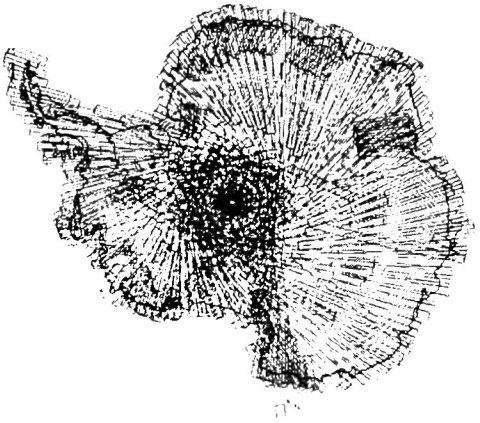

Figure 4. AIC Nominal Plan

An additional opportunity was realized because of the early start on September 19. Radar data, collected after the conclusion of the nominal mission, were acquired exactly 24 days after the beginning of the early start data. This schedule repositioned the spacecraft to within a few hundred meters of its position 24 days earlier. Consequently the data are suitable for interferometric analysis – a demonstrated technique for estimating ice sheet surface topography and surface displacement. Exact repeat data collections started on October 14 and continued through October 20. A map of exact repeat data is shown in fig. 5. During this period 1 pass of scan sar data was also acquired over the area south of 78 degrees latitude.

Preparations to return the satellite to normal operations began on October 20. Arctic mode operations resumed on October 23. Acquisitions for customers resumed on October 26. This occurred 9 days ahead of the planned schedule.

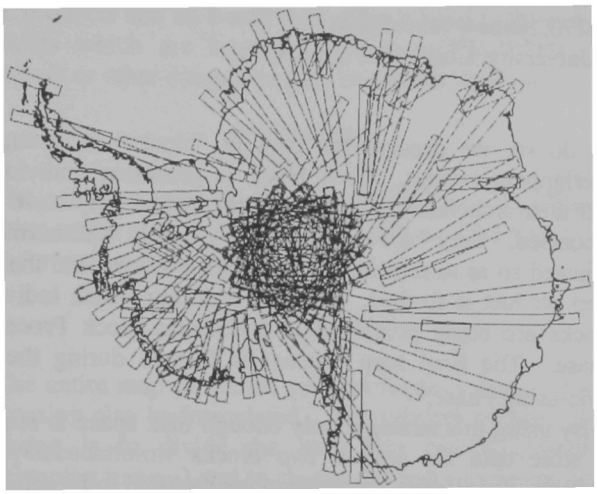

Figure 5. Interferometric Coverage

SCIENCE LESSONS LEARNED FROM AMM-1

Key science lessons learned from AMM-1 included verification that September/October timing for AMM-1 was optimal[4]. There was no evidence for surface melting which means that subsequent mappings at the same time of year will better discriminate between long term glaciologic changes and more ephemeral meteorological variations. Timing also proved good for studying coastal processes such as polynas which were easily delineated within the winter sea ice pack. All Radarsat beams provided excellent definition of surface structure. Ascending Standard Beam 2 proved a good choice for collecting data. The fact that the radar passed over the ice sheet onto the ocean also seems to have mitigated automatic gain control artifacts. Extended high-beam 4 data-acquisitions were originally planned to occur only over the southernmost portion of the continent. In fact, passes were acquired from the coast to the pole and data analyzed so far are excellent. This is somewhat surprising because volume scattering from the ice sheet is presumed to be the dominant electromagnetic process initially suggesting that shallow incidence angle beams would be insensitive to the slight topographic variations across the ice sheet. Finally, initial successes to create interferograms and derive surface velocity data are encouraging [5]. Interferometric studies of different areas are needed to determine how effective a 24-day repeat cycle will be for extensive ice motion measurements.

PLANNING FOR AMM-2

The Radarsat Antarctic Mapping Project calls for two complete Antarctic Mapping Missions, goals that are embraced by the Canadian Space Agency, NASA and the Antarctic Science community. Originally, the mapping missions were envisioned to be nearly exact duplicates to highlight change detection studies of the ice sheet. In view of the success of the AMM-1 and the more complete understanding of the potential value of these mapping opportunities, the planning for AMM-2 is being revisited.

Planning for AMM-2 will concentrate on 5 broad goals based on lessons from AMM-1. These are:

1) Establish a second benchmark for change detection studies (3 to 5 year mapping intervals).
2) Increase the overall science payoff through coordination with other complementary programs (IceSat, ERS, ENVISAT).
3) Exploit lessons learned from AMM-1 to highlight Radarsat unique science capabilities (e.g. INSAR for latitudes south of 78 degrees).
4) Develop a strategy for north mode data acquisitions to complement AMM-2
5) Encourage broader scientific participation in AMM-2 through the distribution of data from AMM-1.

ACKNOWLEDGMENTS

This work was supported by NASA and under a cooperative agreement with the Canadian Space Agency. Data were processed by the Alaska SAR Facility.

REFERENCE

[1] Jezek, K. C. and F. D. Carsey, 1993. RADARSAT: The Antarctic Mapping Project. *BPRC Report No. 6*, 24 p.

[2] Jezek, K.C., J. Curlander, L. Norikane, F. Carsey, J. Crawford, C. Wales, J. Muller, 1996. RADARSAT: The Antarctic Mapping Project. . Proceedings IGARSS'96. Lincoln, NE, p.1775-1776.

[3] Norikane, L., B. Wilson, K.C. Jezek, 1996. RADARSAT Antarctica Mapping System: System overview. Proceedings IGARSS'96. Lincoln, NE, p.1772-1774.

[4] Jezek, K.C., H.G.Sohn, K.F. Noltimeir, in press. The Radarsat Antarctic Mapping Project. IGARSS'98, Seattle, WA.

[5] Forster, R., K. Jezek, A.L. Gray, K. Matter, and H. Sohn, in press. Analysis of Glacier Flow Dynamics from Preliminary Radarsat INSAR Data of the Antarctic Mapping Mission. IGARSS'98, Seattle, WA.

RADARSAT Antarctica Mapping System: System Overview - An Update

Lynne Norikane[1], Bob Wilson[1], and Ken Jezek[2]

1. Vexcel Corporation 4909 Nautilus Ct., Boulder, Colorado 80301
(303) 444-0094, Fax: (303) 444-0470, lynne@vexcel.com
2. Byrd Polar Research Center, Ohio State University, Columbus, Ohio 43210

Abstract -- In October 1997, RADARSAT mapped the entire Antarctic continent from space, presenting scientists with an unprecedented snapshot of the entire continent in the microwave spectrum. NASA has charged the Byrd Polar Research Center with the goal of producing a full continental map using this data, subject to a number of constraints to maximize the utility of the data to the scientific community. To meet these requirements, a number of SAR data processing techniques shall be applied including orthorectification processing, block adjustments for ephemeris refinements, simulation techniques and radiometric balancing for automated image seam removal. These techniques are implemented in the RADARSAT Antarctica Mapping System developed by Vexcel Corporation for the Byrd Polar Research Center. In this paper, we will provide an overview of the system and preliminary results obtained by processing data from the Antarctic Mapping Mission.

OVERVIEW

Over the course of 31 days in September and October of 1997, over 30 hours data were collected by the Canadian RADARSAT sensor, completely mapping the continent of Antarctica. These data in turn will be processed by the Alaska SAR Facility (ASF) into at least 3600 image frames, all to be ultimately assembled into a single digital mosaic by the Byrd Polar Research Center (BPRC). To form this mosaic, Vexcel Corporation has developed the RADARSAT Antarctica Mapping System (RAMS) which is specifically designed to handle the large data volumes and demanding processing requirements for this project.

RAMS consists of a combination of hardware and software solutions. It resides on one or more Unix platforms. The choice and number of platforms used is highly dependent on the desired overall throughput for map formation. The data processing software are accessible via graphical user interfaces (GUIs) which are written in C and XWindows. Both data processing software and GUIs interface to a database and operate on other files such as images.

PROCESSING STRATEGY

The overall processing strategy for map formation is designed to handle both large data volumes (more than can be stored on disk simultaneously) and to allow map formation to begin prior to all data being processed into images by ASF. To do so, we process the data in "blocks" or groups of overlapping images. Each block is processed individually and then archived. After all blocks for the map have been processed, they are geometrically and radiometrically adjusted so as to remove block-to-block seams, and the final map product is formed. The phase during which individual blocks are being processed is called the Block Processing Phase. The final map product is formed during the Tile Processing Phase.[1]

By using this strategy, only enough disk space is required to store data for one or two blocks simultaneously. In addition, not all data for the map are required to be processed by ASF before map formation can begin. An overview of the system is shown in Figure 1. Each of the data processing steps shown are described in more detail later.

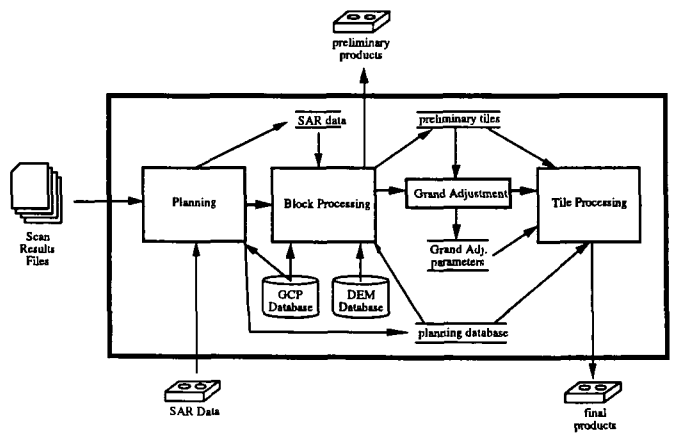

Figure 1: RAMS Data Processing Overview

PLATFORM

The overall performance and number of platform(s) needed are a function of the overall throughput requirement for map formation. Using today's mid-range computing systems, it is clear that multiple platforms or CPUs are required to meet BPRC's requirement to form one map within 15 months.

In addition to one or more computer platforms for RAMS, a variety of additional peripheral devices are required. A large disk array is needed to store input and output images,

[1]The actual map product consists of approximately 90 individual tiles which are each divided into 75-115 smaller sub-tiles.

digital elevation maps (DEMs) and ground control points (GCPs), intermediate products, and the RAMS database. RAMS currently contains a 64 GB disk array. To backup and restore data to the disks, a backup system is required (such as a digital linear tape (DLT)). The DLT is also used to ingest ASF products and an 8-mm tape drive is used to save output products which are later mastered onto CD-ROMs. X-terminals or other computers may be used as displays.

SOFTWARE

The software components of RAMS are best described in relation to the overall data processing flow. The first step in map formation is processing planning.

Processing Planning

The entire map formation process requires that an overall processing plan be formulated. The primary purpose of this planning is to divide the map into blocks (groups of overlapping images) and to choose the order in which blocks will be processed. Given this, data processing requests must be submitted to ASF in the proper sequence. After the first data have been received, Block Processing may begin.

A good block is considered to have the following characteristics. At least 2 radar-visible ground control points must be contained within its boundaries. Blocks should consist of long contiguous swaths of data, overlapping each other in the cross-track direction.

Block Processing

Once all data for a given block have been received, block processing may begin. The overall objective is to combine all image frames for the block into preliminary map tiles. The result must satisfy geometric and radiometric accuracy requirements and must be seamless in appearance.

The first objective is to compute a block adjustment or correction to all orbits contained within the block. To do so, we require the collection of ground control points and tie points between frames within the block.

Tie Points Tie points are collected in both an automated fashion and a manual fashion. Tie points are collected in the along-track direction through an automated process. Cross-track tie points (i.e. tie points collected between frames in different orbits) are also collected in an automated fashion using estimates on locations of overlap regions and an image automatcher.

The operator may choose to verify or correct the automatcher results and may choose to manually select new tie points.

GCPs Ground control points must be manually located by the operator. At least 2 GCPs are required per block

Block Adjustment Given a sufficient number of tie points and located ground control points within the block, the block adjustment may be computed. In this step, the block adjustment corrects all orbits within the block such that tie points are reconciled as closely as possible and GCPs are geolocated as accurately as possible. The overall goal is to greatly exceed the 300 meter geolocation accuracy requirement for the map.

Orthorectification Once the block adjustment has been computed, all image frames are resampled into a map grid, taking into account geometric distortions due to terrain. Radiometric corrections due to slope effects are also applied in this step.

Radiometric Balancing The next step is to remove radiometric seams between images in an automated fashion. This is done by taking advantage of our already having tie points between images. At each tie point, local image statistics are computed and a target value assigned. Using actual and target values at each tie point, a radiometric balancing function may be computed as a function of image position. One such function is computed for every image in the block.

Preliminary Tile Formation The final step in block processing is to apply the radiometric balancing functions to the orthorectified images and form preliminary map tiles. Having done so, image chips are extracted around the block edges for later use during the Grand Adjustment. The operator may also choose to create preliminary products. Otherwise, the data is archived, the disk is cleaned, and data loaded for the next block.

Options If data were collected for the purposes of filling in areas of layover or shadover, a steps are required to reset these areas and merge the orthorectified data collected for that purpose.

Grand Adjustment

Once all blocks have been processed individually, the Grand Adjustment is performed. In this step, the radiometric and geometric seams between blocks are removed. To do so, the block-to-block image chips collected during block processing are used to compute tie points and their local image statistics.

The radiometric balancing approach is essentially the same as that used for individual blocks. The geometric adjustment computes an offset and rotation for each block. based on the block-to-block tie points.

Tile Processing

The formation of the final map products are done during the tile processing phase. In this phase, the results of the Grand Adjustment are applied to each block in turn. These data are then merged into final tile products which can then be prepared for CD-ROM mastering. In addition, overview or lower-resolution map products may be formed for areas of larger extent.

OPERATOR INTERFACES

Throughout RAMS, the operator initiates processing and can view and often modify intermediate results through graphical user interfaces. RAMS is an exceptionally flexible system. The operator can be guided through the various processing steps or may choose to beat his or her own path.

BATCH PROCESSING

RAMS relies on overnight batch processing to meet overall throughput requirements for map formation. An intelligent program dispatcher is used to control both the order in which programs are run and the number of programs which may run simultaneously on one or more different platforms. The dispatcher has its own GUI which provides the operator with a list of pending jobs, jobs currently being run, and jobs completed. Access to error logs is also provided.

PRELIMINARY RESULTS

Shown in this Figure 2 is the first radar composite image of McMurdo Dry Valleys. The dry-valley region of Victoria Land is a cold desert that is essentially snow free and interrupted by alpine glaciers. The valleys are protected from ice flooding from the East Antarctic Ice Sheet by the Transantarctic Mountains which flank the valleys to the west. In the lower reaches of the valleys, melt water flows along the glaciers feeding the many small lakes and ponds that are found here. The U.S. National Science Foundation has established a Long Term Ecological Research site in the McMurdo Dry Valleys for monitoring this fragile environment. The cold, dry conditions of the valleys also serve as such a good analogue for the Martian environment that NASA has tested there equipment and experiment concepts in anticipation of Martian exploration.

The upper left portion of the mosaic includes the outflow of the Koetlitz Glacier. The Bowers and Wilson Piedmont Glaciers are found along the coast and the adjacent sea ice covered waters. Cape Roberts, site of an offshore marine sediment coring program, is located in the lower center of the image. The flanks of the East Antarctic Ice Sheet are seen in the upper right portion of the mosaic.

The Vexcel developed RAMS system will be used to create a complete mosaic of Antarctica comparable in quality to the sample shown. It will take approximately 1.5 years to complete the mosaic making it available for use by the science community in late 1999.

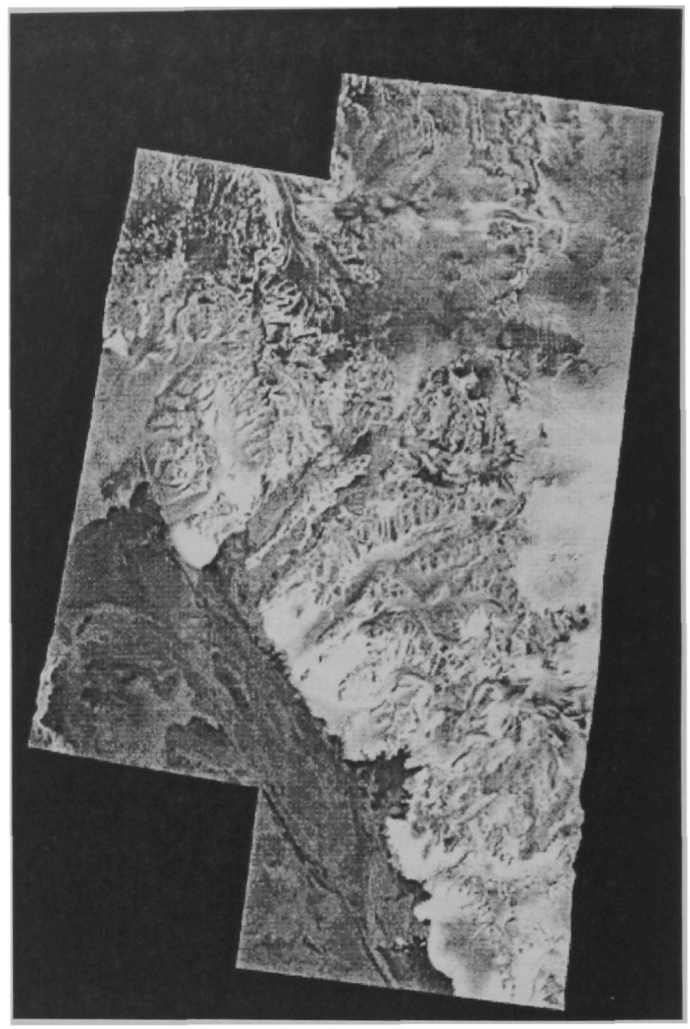

Figure 2: McMurdo Dry Valleys

SUMMARY

RAMS is a complete end-to-end processing system for the formation of large-scale maps from synthetic aperture radar imagery. It utilizes the techniques of block adjustment for improving geolocation accuracy, orthorectification for terrain distortion removal, automated radiometric balancing for image seam removal, as well as other techniques to improve the overall quality of the final product, at the same time, providing the operator with a large degree of control over each step to ensure the formation of the best product possible. Preliminary results indicate that the final mosaic will provide many insights leading to scientific discovery.

REFERENCES

[1] Jezek, K. C., and F. D. Carsey, 1993. Radarsat: The Antarctic Mapping Project. Byrd Polar Research Center Report no. 6, 24.

THE RADARSAT ANTARCTIC MAPPING PROJECT

K.C. Jezek, H.G. Sohn, and K.F. Noltimier

Byrd Polar Research Center
1090 Carmack Road
The Ohio State University
Columbus, OH 43210
(jezek@iceberg.mps.ohio-state.edu)

INTRODUCTION

During September and October 1997, the Canadian Radarsat-1 was used to successfully acquire the first, high-resolution synthetic aperture radar image data set of the entire Antarctic Continent. This unprecedented activity was made possible by the in-orbit rotation of the SAR to look towards the South Pole and the electronic beam steering capability of the instrument to image to the Pole. These attributes, combined with the ability to operate day or night and to penetrate cloud, provide a nearly instantaneous snapshot of the southern continent.

A composite mosaic constructed from over 3000 Radarsat-1 frames processed immediately after the mission by the Alaska SAR Facility is shown in Fig. 1. These Quick-look images were processed throughout the Antarctic Imaging Campaign (AIC) on the Jet Propulsion Laboratory designed Alaska SAR Processor. Quick-look images are 100 km on a side, are not radiometrically or geometrically calibrated and, in this case, have 100 m pixel size. The images were originally intended to verify that swaths overlapped at the coast and to visually verify data quality as it might be used to make real time changes in the acquisition plan. In fact the composite reveals extraordinary details about the glaciologic and geologic structure of the Antarctic. It is indeed a new view of Antarctica and provides for a quantitative analysis of surface properties over all of East and West Antarctica (Fig. 1 and 2).

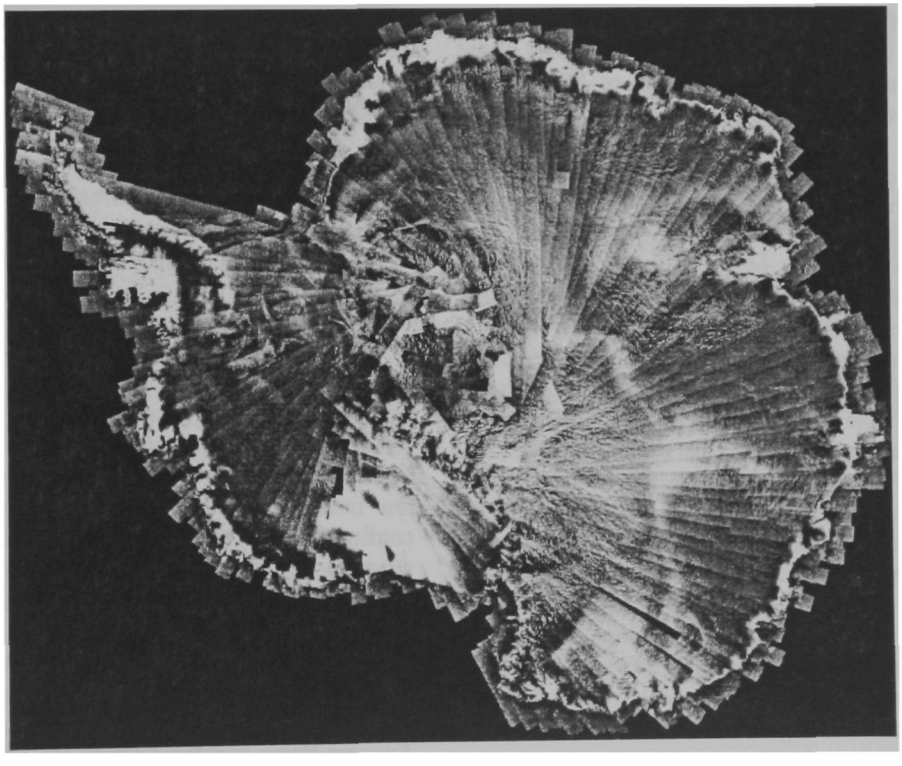

Figure 1. Synthetic Aperture Radar Mosaic of Antarctica. Data were acquired by Radarsat-1 during September and October 1997.

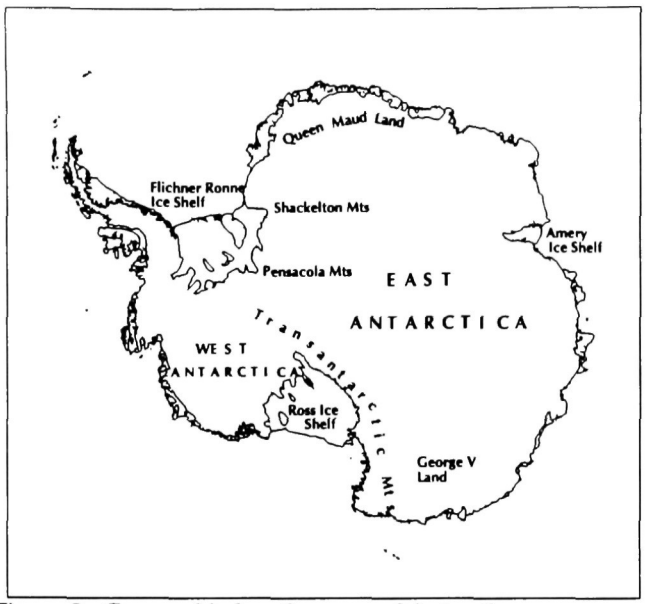

Figure 2. Geographic location map of Antarctica

DISCUSSION

We observe several new and exciting features about Antarctica from the mosaic (Fig. 1). First, there are large-scale spatial variations in radar brightness. Many of the thousands of kilometer long curvilinear features across East Antarctica appear to follow ice divides separating some of the large catchment areas. The bright portion of Marie Byrd Land in West Antarctica and the eastern sector of the Ross Ice Shelf probably represent the region where significant melting and refreezing occurred during an early 1990's melt event. Most of the coastal areas and much of the Antarctic Peninsula appear bright also because of summer melt. But unlike Greenland, where most of the large-scale brightness patterns are associated with firn melt facies, the remaining, strong variations in radar brightness are poorly understood.

On an intermediate scale, the East Antarctic Ice Sheet appears to be very 'rough'. The texturing is probably primarily due to the flow of the ice sheet over a rough glacier bed. Textures are particularly strong paralleling the flanks of the Transantarctic, Pensacola and Shackelton Mountains and extending deep into adjacent portions of the East Antarctic Plateau. Long linear patterns are strongly suggestive of subglacial geology and may indicate that the ice sheet in this area is resting on relatively resistant basement rocks. The texture changes abruptly across the northernmost section of the Wilkes Subglacial Basin located in George V Land. There the imagery shows remarkable subtle rounded shapes similar in appearance to the signature of subglacial lakes such as Lake Vostok.

Wind driven surface and ice driven processes are manifest at all scales across the mosaic. Extensive dune fields are observed across East Antarctica. The dunes have wavelengths of several kilometers and may be 40 kilometers in length.

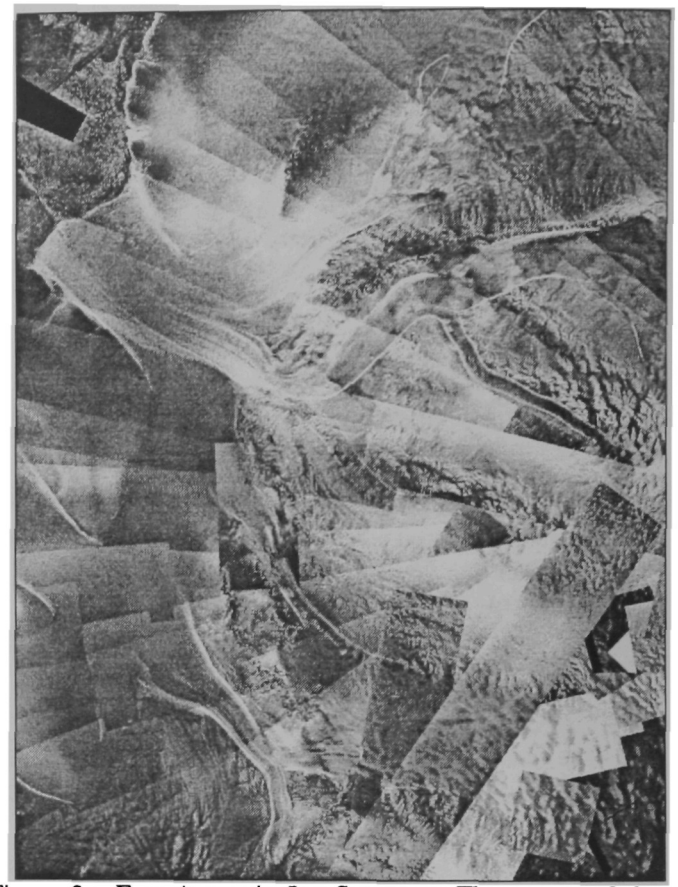
Figure 3. East Antarctic Ice Streams. The center of the image is located at about 82° S. 35.4° W. The image is 880 km wide.

Most intriguing are the ice stream and ice stream like features in Queen Maud Land made visible by the intense crevassing along the shear margins. Slessor Glacier is located in the upper middle portion of Fig. 3. The upper reaches of the glacier are funnel shaped, channeling ice downwards towards the Filchner Ronne Ice Shelf which occupies most of the left of the figure. The northern most shear margin is about 230 km long from the grounding line to the upstream area that seems to be characterized by recently initiated or relict ice stream flow. An enormous ice stream, reaching at least 550 km into East Antarctica, feeds Recovery Glacier. The confluence of a thin, elongated, 270 km-long tributary ice stream with Recovery Glacier is located approximately 250 km from the constriction where Recovery Glacier enters the Filchner Ronne Ice Shelf. The main body of the tributary is crevasse free indicating that shear stresses are concentrated only at the margins. A less active tributary merges with Recovery Glacier just upstream of the grounding line. Support Force and Foundation Ice Streams are located in the lower middle of the image. The upglacier portion of Foundation Ice Stream forks into two tributary streams that extend about 180 km into East Antarctica. Taken together, these East Antarctic Ice Streams are significantly more

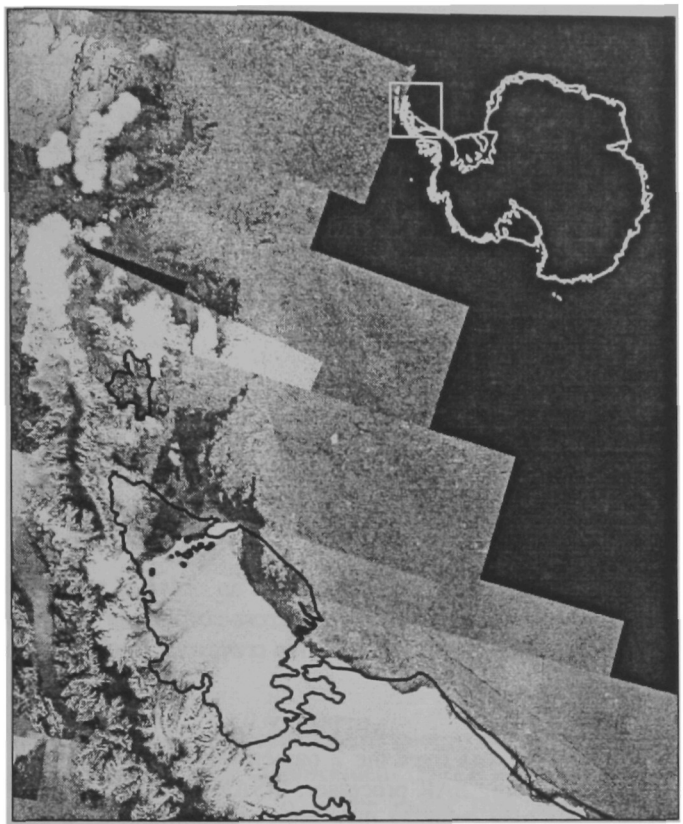

Figure 4. Portion of the Antarctic Peninsula showing the region that formerly contained the Northern Larsen Ice Shelf. The dark tones offshore of the Peninsula and remaining Larsen Ice Shelf are indicative of coastal polynas. The black line shows the grounding line and the former seaward extent of the ice shelf.

extensive than the more studied West Antarctic Ice Streams. The presence of the ice stream system also suggests more active mechanisms for moving ice out of the East Antarctic Ice Sheet – perhaps indicating a potentially more changeable ice sheet than previously imagined.

Finally, the grounded and floating margins of the ice sheet are clearly discernable in Fig. 1. Initial inspection and comparison with historical data sets (such as the British Antarctic Survey Antarctic Digital Database) suggests that there are no systematic patterns of ice margin advance or retreat. For example, the ice fronts of the Ross and Amery Ice Shelves have advanced since the mid-1980's. As documented by several authors, the northern Larsen Ice Shelf experienced nearly catastrophic retreat in 1995 (Fig. 4). Interestingly, the ocean region formerly covered by the northern Larsen Ice Shelf is now covered by either very thin ice or by open ocean – both conditions indicative of southern ocean polynya formation. The areal extent of the new thin ice region is about 9630 km^2. The presence of either open water or thin ice contributes a new source of heat flux from the coastal ocean into the local environment.

SUMMARY

Preparation of a radiometrically calibrated and geometrically accurate mosaic is proceeding under the Radarsat-1 Antarctic Mapping Project [1, 2, 3]. The final, seamless, digital mosaic will be produced at 25 m pixel size and be distributed on CDROM. The mosaic will be available for use by the science community in late 1999.

ACKNOWLEDGMENTS

This work was supported by NASA and under a cooperative agreement with the Canadian Space Agency. Data were processed by the Alaska SAR Facility.

REFERENCES

[1] Jezek, K. C. and F. D. Carsey, 1993. RADARSAT: "The Antarctic Mapping Project". BPRC Report No. 6, 24 p.

[2] Jezek, K. C., J. Curlander, L. Norikane, F. Carsey, J. Crawford, C. Wales, J. Muller, 1996. "RADARSAT: The Antarctic Mapping Project"." Proceedings IGARSS'96. Lincoln, NE, p.1775-1776.

[3] Norikane, L., B. Wilson, K. C. Jezek, 1998. "RADARSAT Antarctic Mapping System: System Overview-An Update". Proceedings IGARSS'98, Seattle, WA.

InSAR Results from the RADARSAT Antarctic Mapping Mission Data: Estimation of Glacier Motion using a Simple Registration Procedure

A.L. Gray, K.E. Mattar, and P.W. Vachon,
Canada Centre for Remote Sensing,
588 Booth Street, Ottawa, Canada K1A 0Y7.
Tel: (613) 995-3671, Fax: (613) 947-1383, Email: laurence.gray@geocan.nrcan.gc.ca
R. Bindschadler,
NASA Goddard Space Flight Center, ms 971
Greenbelt, Maryland, USA 20771.
K.C. Jezek and R. Forster,
Byrd Polar Research Center, Ohio-State University,
108 Scott Hall, 1090 Carmack Road,
Colombus, Ohio, USA 43210
J.P. Crawford,
Jet Propulsion Laboratory, 4800 Oak Grove Drive,
Pasadena, California, USA 91109-8099.

ABSTRACT

An interferometric method is used to derive ice motion from RADARSAT data collected during the Antarctic Mapping Mission. Although one cannot solve for both topography and ice motion using one interferometric pair, it is possible to use a coarsely sampled digital terrain model to estimate ice motion using an image registration method. Less accurate than the usual fringe counting method for estimation of radial displacement, the image registration method allows useful motion estimation in both range and azimuth. The method is described and some results shown for a large area (~17,000 km^2) including ice flow into the Filchner Ice Shelf.

INTRODUCTION

During September and early October 1997, RADARSAT was manoeuvred to operate in a left looking mode and carried out the first high resolution mapping of the complete Antarctic continent. The RADARSAT satellite is in a 24 day repeat orbit and it was suspected that this time period was too long to expect satisfactory coherence, especially for coastal outflow glaciers [1]. However, in interior Antarctica, surface snow or ice melt is very rare. Therefore, there was a possibility that backscatter from the firn and upper ice layers would not change sufficiently in the 24 days between data acquisitions to destroy the necessary coherence for interferometric analysis. The data were collected as part of the Antarctic Mapping Mission (AMM) organized as a result of the NASA/CSA agreement whereby NASA launched RADARSAT in exchange for access to data and the opportunity to map Antarctica. During the last 6 days of the 30 day mission, the coverage of the first 6 days was repeated exactly, thereby generating many pairs of images with which this type of interferometric analysis is possible. The technique used to measure the ice motion is an image correlation approach and depends on the coherent speckle pattern in the 2 images being correlated. The accuracy with which registration can be achieved is an order of magnitude better than with the incoherent cross-correlation approach that depends on image features, like crevasses, to obtain good results.

METHOD

Raw signal data from the 2 passes were processed with a phase preserving SAR processor, dtSAR, supplied by MDA. The single look complex data were oversampled by a factor of 2 in both range and azimuth prior to detection. To avoid aliasing problems with the sin(x)/x kernel used in the oversampling, the azimuth frequency was shifted to be centred on zero Doppler using the Doppler centroid information. After detection, image chips were cross-correlated to obtain the offset in both azimuth and range. The cross-correlation function was then oversampled by an additional factor of 20 in both directions. The position of the peak in the oversampled cross-correlation function was used to determine the pixel shifts and the magnitude was used as a quality factor for poor point rejection. The pixel shifts in image slant range (δ_r) and image azimuth (δ_a) can be related to the 24 day ice displacements in the ground range (D_r) and azimuth (D_a) directions through the relations:

$$\delta_r = B\, cos\,(\chi - \alpha) + D_r\, sin\,(\theta + S_r) \qquad (1)$$

and

$$\delta_a = D_a\, cos\,(S_a) \qquad (2)$$

where the baseline, angle, and slope parameters are defined in Fig. 1. For the baselines estimated for these data, typically less than 200 m, the error associated with the parallel ray approximation implicit in (1) is only a few centimetres, small in comparison with other errors. Knowledge of the baseline is required, as well as a digital terrain model for calculation of the incidence angle, look angle, and terrain slopes.

In practice, it is normally possible to use 1 or 2 points in the imagery, which correspond to exposed rock or mountains, to help calibrate the ice displacement information. Radar look and incidence angles are calculated for points in the digital

terrain model by using the satellite orbit information and solving for the zero Doppler range between the point on the

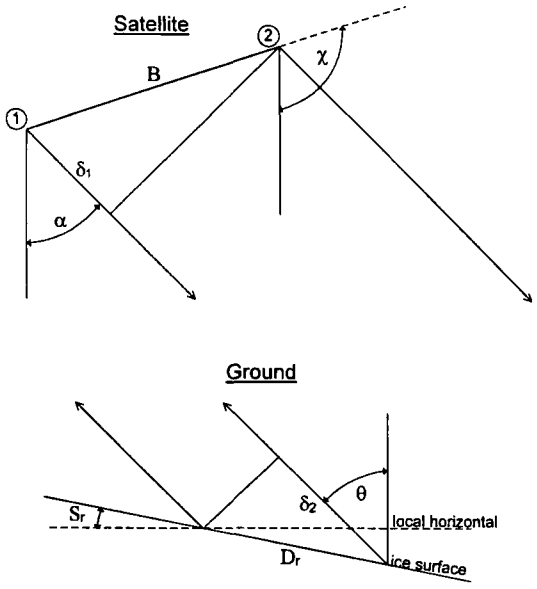

Fig. 1
Illustration of the displacement geometry for calculation of the ground range displacement (D_r). B is the baseline, χ is the baseline angle, α is the radar look angle at the satellite, S_r and S_a are the terrain slopes in range and azimuth respectively (to the local horizontal), θ is the local incidence angle, and $\delta_r = \delta_1 + \delta_2$.

earth's surface and the satellite track. The orbit data are used to get an initial estimate of the baseline B and the baseline angle χ. The baseline information is refined using the zero velocity points.

A complete error analysis is beyond the scope of this paper but the following points can be made. The pixel registration in areas of good coherence can be done to better than 1/10 of a pixel, the 'unit' of pixel shift in this work is 1/40 of the pixel spacing. Small bias errors in velocity may exist when using an area that is assumed to be stationary. These errors can increase with both baseline and the look angle difference between the reference area and the area for which the velocity estimate is being made. It is anticipated that errors in velocity will be in the range of 10 cm/day in range and around 3 cm/day in azimuth. With poor digital elevation data, or poor baseline information, these errors will increase. Absence of a 'zero velocity' reference area will make the technique more difficult, and the results more uncertain, however it is anticipated that velocity gradients will still be measurable.

RESULTS

Figure 2 illustrates the ice movement derived from two merged pairs of RADARSAT standard mode 2 images (100 km x 170 km) acquired on September 24 and October 18, 1997. The vectors represent the ice motion of the Slessor Glacier as it flows into the Filchner Ice Shelf in Western Antarctica. The vector direction corresponds well with the flow lines in the glacier and, as the range and azimuth displacement estimates are independent, the agreement between the derived directions and the ice stream flow lines helps validate the derived velocities. The acceleration in the ice stream as it enters the floating ice shelf is apparent. Velocities in the more southerly (upper) part of the glacier change from around 250 m/year as the ice enters the area covered by the image to almost 800 m/year as it leaves at the bottom right-hand corner.

CONCLUSIONS

In 24 days time ice displacement can be large enough that a simple image registration technique can lead to useful results for ice motion. The advantages are:

- Displacements in both range and azimuth can be measured.
- Phase analysis is not essential, so that errors due to phase aliasing or incorrect phase unwrapping are avoided.
- Local errors do not propagate through the image as they can with phase analysis.
- In some cases, use of the phase information could be used to improve the range velocity or velocity gradient estimation.
- The accuracy requirements for orbit and terrain topographic data are not as stringent as for conventional interferometric analysis for terrain motion.

ACKNOWLEDGMENTS

Dirk Geudtner (DLR) provided help and software for our early work on RADARSAT interferometry. The Canadian Space Agency, CSA, and RADARSAT International, RSI, also helped in making data available to CCRS in order to do an initial evaluation of the potential of interferometry.

REFERENCE

1. Goldstein, R.M., H. Englehardt, B. Lamb, and R.M. Frolich, Satellite radar interferometry for monitoring ice sheet motion: Application to an Antarctic ice stream, *Science*, 262, 1525-1530, 1993.

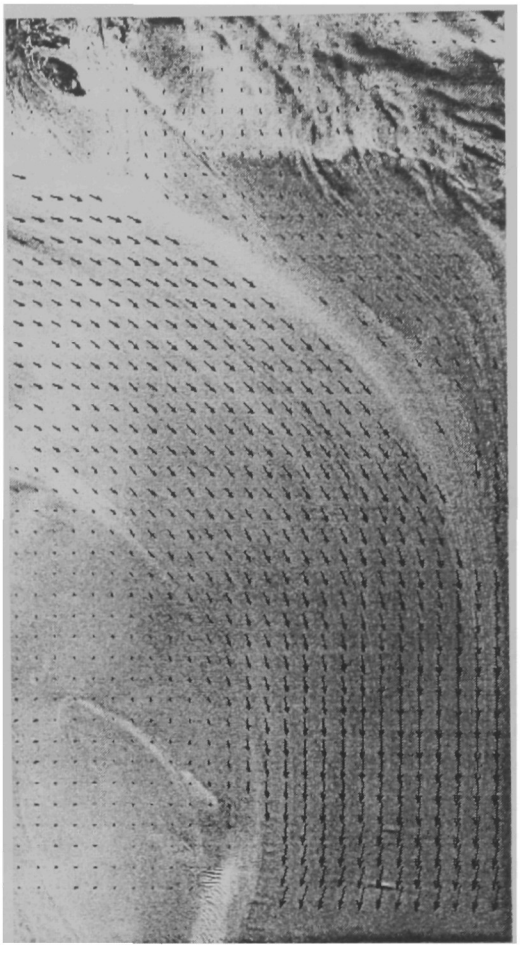

Figure 2
Illustration of ice motion from the Slessor Glacier (upper left) as the ice enters the Filchner Ice Shelf and flows as an ice stream northward towards the shelf edge. Two mosaicked pairs of RADARSAT standard mode 2 images were used to create this image (100 km x 170 km) of ice motion. Velocities in the more southerly (upper) part of the glacier change from around 250 m/year as the ice enters the area covered by the image to almost 800 m/year as it leaves at the bottom right-hand corner.

Analysis of Glacier Flow Dynamics from Preliminary RADARSAT InSAR Data of the Antarctic Mapping Mission

Richard R. Forster, Kenneth C. Jezek, Hong Gyoo Sohn
Byrd Polar Research Center, The Ohio State Universtiy
1090 Carmack Rd., Columbus, OH 43210
tel. (614)292-1063, fax: (614)292-4697, forster@iceberg.mps.ohio-state.edu

A. Laurence Gray and Karim E. Matter
Canada Centre for Remote Sensing
588 Booth St., Ottawa, Ont., Canada K1A 0Y7
tel. (613)995-3671, fax: (613)947-1383, laurence.gray@geocan.nrcan.gc.can

INTRODUCTION

The entire continent of Antarctica was mapped at a 25-meter resolution with synthetic aperture radar (SAR) during the Radarsat Antarctic Mapping Project (RAMP) over a 30-day period in the fall of 1997 providing a static "snapshot" of the ice sheet [1]. Since Radarsat-1 has a 24-day orbit cycle, repeat-pass interferometric SAR (InSAR) data was also acquired. The extensive InSAR data [1,2] will provide a view of ice sheet kinematics, for use in studies of glacier dynamics over vast unexplored areas. This information is required to determine the response of the Antarctic Ice Sheet to present and future climate change. In this paper we present the results of analysis of an InSAR pair for the Recovery Glacier, East Antarctica.

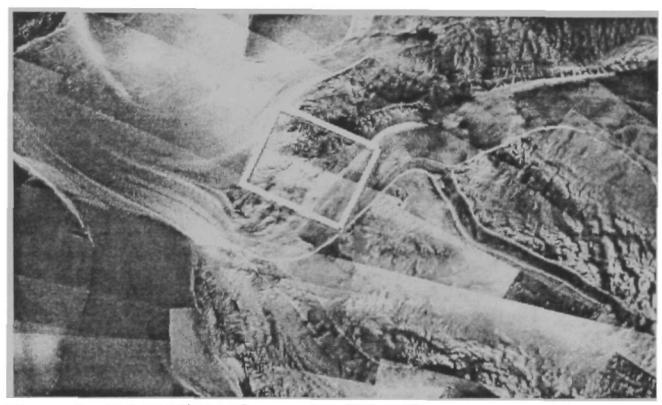

Figure1. RADARSAT mosaic of the East Antarctic Ice streams centered on Recovery Glacier. Box is InSAR scene

RECOVERY GLACIER

The Recovery Glacier is a major outlet draining a portion of Queen Maud Land to the Filchner Ice Shelf. Feeding the glacier is a large ice stream and tributaries, the extent of which, are easily observable from the RAMP mosaic (Fig. 1) [3]. The shear margins are well delineated by the strong returns from the intense crevassing. The InSAR scene (Fig. 2) straddles both of Recovery Glacier's lateral shear margins. The main trunk of this part of the ice stream is contained in the lower third of the image. Radarsat-1 (λ = 5.66 cm) imaged the area on Sept 24 and Oct. 18, 1997 from ascending orbits with a 28° look angle.

Figure 2. Amplitude image of Recovery Glacier Ice Stream. The width is 100 km and illumination is from the left

INTERFEROMETRY

The single look complex pair was processed at CCRS with a range and azimuth spacing of 8.12 and 5.37 m respectively. The interferogram was produced using 3 range and 10 azimuth looks resulting in approximately 50 m pixels (Fig. 3).

The coherence (Fig. 4) is remarkably high for most of the area considering its dynamic nature coupled with the 24-day repeat. The lateral shear margins are clearly evident as the wide linear bands of very low coherence caused by large differential motion and/or rotation within the crevasse zones. The high coherence of the main ice stream was obtained by allowing for additional pixel offsets for this portion of the image. The bright bands orthogonal to the flow direction on

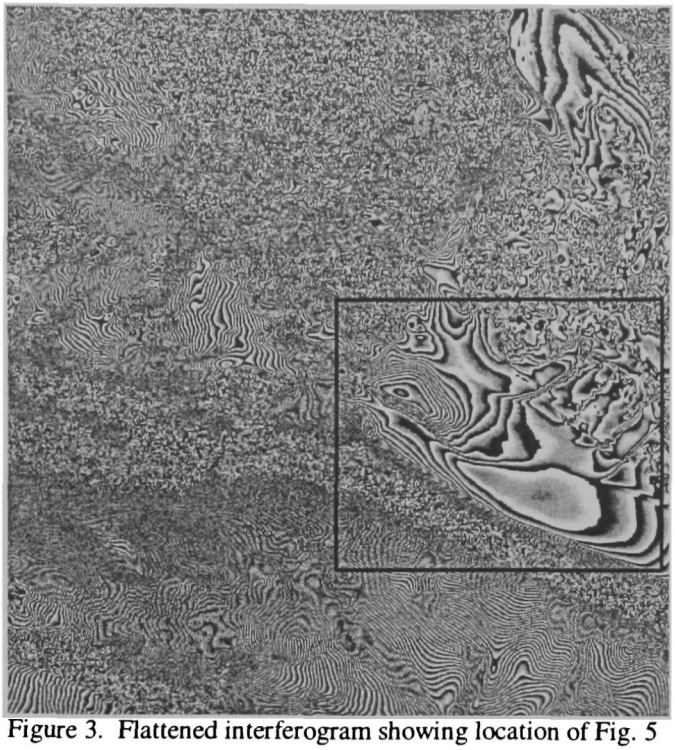

Figure 3. Flattened interferogram showing location of Fig. 5

Figure 4. Coherence map with strain rate transect.

the lower right of the main trunk have a wavelength of 5 km and are not evident on the amplitude image (Fig. 2). We suspect that subtle topographic undulations are causing these fluctuations in coherence possibly due to the vertical displacement variability. This is also suggested by the tightly curving phase lines (Fig. 3). If the pattern were caused by slight scattering differences associated with topography it is likely it would be observable on the amplitude image as well. The rumpled texture in the upper central portion of the image also appears in the amplitude image but with much less contrast. We interpret this as another example of subtle ice sheet topography detected with the phase coherence map.

The grounding line also appears to be detectable in both the amplitude (Fig. 2) and coherence images (Fig. 4). It is delineated by the abrupt change of intensity at the very top of the amplitude image and can be traced as a more subtle line back to the mountains. The coherence map shows this area as a more diffuse transition to low coherence. Interestingly there is an area of high coherence immediately on the floating side of the grounding line.

The flattened fringe image (Fig. 3) contains contributions from both displacement and topography. However, outside of the Shackleton Range (center right) the area is rather flat leaving the phase to be dominated by displacement. The slower moving ice on the flanks of the mountains is separated from the faster moving central core by the incoherent phase within the northern shear margin.

The phase was initially flattened by removing the dominant fringe rate in the range and azimuth directions. A more precise estimate of the baseline and removal of its effects will be done using ground control points acquired for generating the final RAMP mosaic. The topographic phase component will also be removed using a DEM that is being compiled for terrain correction of the RAMP data.

ICE VELOCITY AND STRAIN RATE

The phase was successfully unwrapped over most of the image using the branch-cut method. The unwrapped phase was scaled by the wavelength converting it to a relative displacement in the radar line-of-sight (LOS). Displacements at rock out-crops were set to zero by adding a constant resulting in an absolute LOS displacement map.

A portion of the LOS velocity map is shown in Fig. 5 over the amplitude image. The extent of the map shown was intentionally limited to areas of coherence > 0.5. The LOS velocities rapidly increase from 1.5 to 8 m/a at the shear margin. This portion of the glacier, along the flank of the Shackelton Range, separated from the main flow by the right lateral shear margin is moving very slowly and appears to be fed only by small mountain glaciers. This corridor of isolated flow extends up glacier for over 200 km along the range. Its ice does not enter the Filchner Ice Shelf through the constriction of the Recovery Glacier instead it widens and enters to the east of the main outlet (Fig. 1). The ice at this point must be very thin.

Figure 5. Radar line-of-sight velocity contours over the amplitude image. Contours range from 0.5 to 8.0 m/a.

This initial LOS velocity map is less reliable for the small mountain glaciers due to topographical influences that will be removed in later versions using our DEM. The LOS velocity can be converted to horizontal ice surface velocities with a DEM and an estimate of flow direction from either the DEM or flow lines that are visible on the amplitude image.

The highly decorrelated lateral shear margins of the ice stream prevent us from tying the relative displacement field to a point of no displacement. However, the relative displacements along with a flow direction can be used to calculate the strain rates. In fact, the phase need not be unwrapped to calculate strain rates.

The longitudinal strain rate for the main trunk along a flow line was calculated directly from the wrapped phase using

$$\dot{\varepsilon} = \frac{dV_f}{dx}$$

$$V = \frac{\phi\lambda}{4\pi}\frac{1}{T} + V_0$$

$$V_f = \frac{V}{\cos\alpha\sin\theta - \cos\theta}$$

$$\frac{dV_f}{dx} = \frac{\lambda}{4\pi}\frac{d\phi}{dx}\frac{1}{T}$$

where V_f is the ice surface velocity in the direction of flow, x is the distance along the transect, V is the radar line-of-sight velocity, ϕ is the wrapped phase, λ is the radar wavelength, T is the time between SAR acquisitions, V_0 translates the relative velocity to absolute, α is the angle between flow direction and cross-track heading, and Θ is the radar look angle.

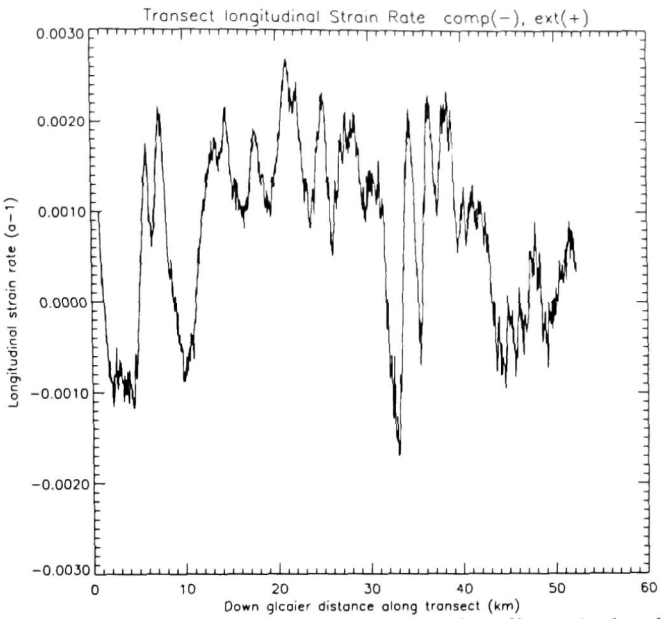

Figure 6. Longitudinal strain rate along a flow line calculated from the wrapped phase of the interferogram. The location of the transect is shown in Figs. 2 and 4.

The results are shown in Fig. 6. The strain rate is predominately compressive with fluctuations at approximately a 5 km wavelength. The locations of change to compressive flow are associated with the bright and dark patterns seen on the correlation map (Fig. 3). This is consistent with their interpretation as subtle topographic features.

SUMMARY

Analysis of the Recovery Glacier data set has demonstrated the excellent quality of InSAR data available from the Radarsat Antarctic Mapping Mission and its application to glacier dynamics. Phase coherence is high over most this highly dynamic area even though the temporal baseline is 24 days. The coherence image enhances subtle ice sheet topography and indicates the location of shear margins and the grounding line. A radar line-of sight ice velocity map identified a large region of slow moving ice that drains the Shackelton Range. Longitudinal stain rates along a flow line within the main ice stream were calculated directly from the wrapped phase.

REFERENCES

[1] Jezek, K., et al., 1998. "Snapshots of Antarctica from Radarsat-1", IGARSS'98, Seattle WA

[2] Gray, A. L., et al., 1998. "Preliminary InSAR results from Radarsat Antarctic Mapping Mission data: Estimation of glacier motion using a simple registration procedure", IGARSS'98. Seattle WA.

[3] Jezek, K. H. Sohn and K. Noltimier, 1998. "The Radarsat Antarctic Mapping Mission", IGARSS'98, Seattle WA.

Flow Variations of the Antarctic Ice Sheet from Comparison of Modern and Historical Satellite Data

Kenneth C. Jezek
Byrd Polar Research Center
The Ohio State University
1090 Carmack Road
Columbus, OH 43210
(jezek@iceberg.mps.ohio-state.edu)

INTRODUCTION

Since 1962, high quality satellite images of the Antarctic have been acquired which cover much of the Southern Continent. The earliest images, from the Corona Program, have only recently become available to the science community [1]. They reveal a rich variety of details about the ice sheet, ice shelves, grounding lines, and rocky areas [2,3,4]. The most recent high-resolution images covering all of Antarctica were collected by the Canadian Radarsat-1 in September and October of 1997 [5,6]. That activity, a collaboration between NASA and the Canadian Space Agency, has resulted in the first, complete, high resolution SAR mapping of the Antarctic. The Radarsat images are also spectacular and graphically portray Antarctic ice streams, outlet glaciers, calving margins, and mountains.

This paper examines how different Antarctic flow regimes have changed over the 35-year interval between Corona and Radarsat. Study areas focus on the Ross Ice Shelf and Crary Ice Rise. The comparison reveals dramatic variations in ice flow, particularly around Crary Ice Rise - an area of long standing glaciological interest because of its potential for retarding upstream flow (fig. 1).

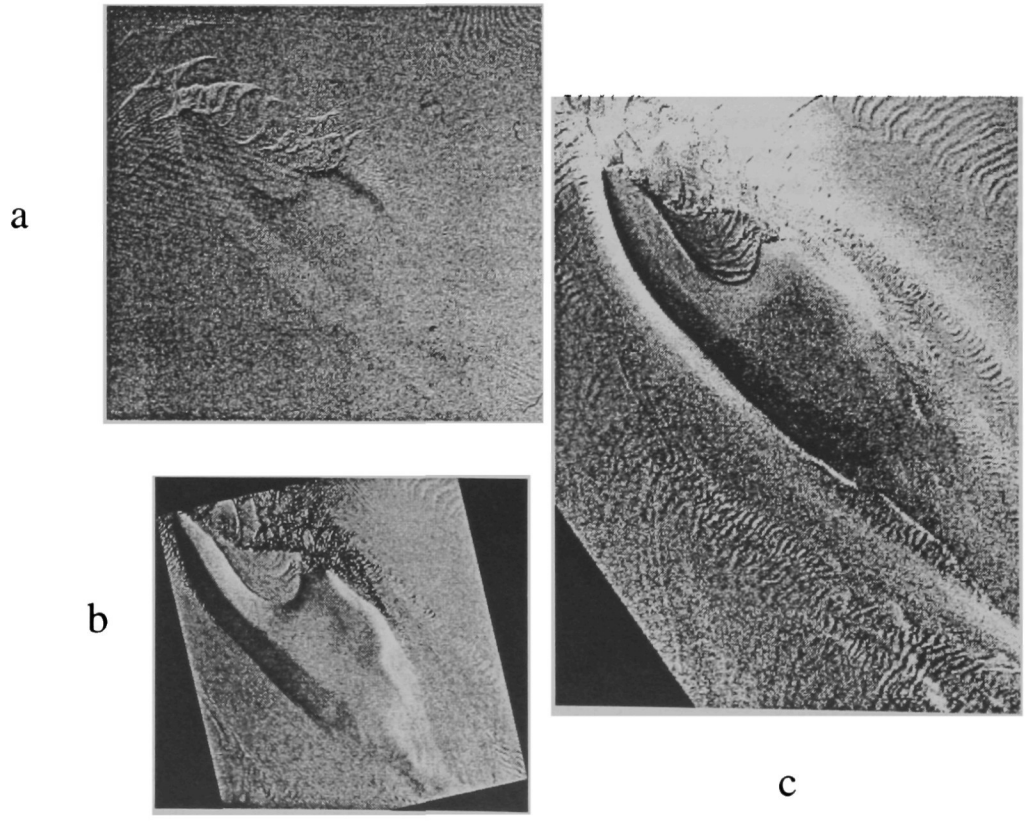

Fig. 1. Crary Ice Rise imaged by three spaceborne sensors: a) Optical Corona satellite imagery from 1963 (DISP); b) SPOT optical imagery from 1995; c) Radarsat synthetic aperture radar microwave imagery from 1997. North is approximately up. In each image, the ice rise is about 24 km wide at its mid-point.

GLACIOLOGICAL SETTING

Crary Ice Rise (83S, 174W) is situated in the southeastern corner of the Ross Ice Shelf, Antarctica. Surrounded by ~ 400 m thick ice floating on the Ross Sea, Crary Ice Rise is an ice capped island that rises nearly 50 m above the adjacent shelf ice. The rise rests in the downstream ice flow from two West Antarctic Ice Streams. As such, some investigators conjecture that the ice rise presents an obstruction to ice flow, effectively damming the upstream ice and contributing to the stability of the inland ice sheet.

More recent studies of the ice rise suggest that Crary Ice Rise is changing - and consequently the effect the ice rise has on local ice flow [7]. Based on ice thickness and ice surface velocity data, the shelf immediately downstream of the ice rise is estimated to be thinning by about 1 m/y. Southwest of the ice stream, the ice shelf is believed to be thickening by a similar amount. These calculations lead to speculation that the location of the ice rise may be shifting. Photographs taken by the Corona Satellite in 1963 and then, 32 years later, by the SPOT Satellite, and most recently by Radarsat-1, support this idea (fig 1).

ANALYSIS

Declassified Intelligence Satellite Program (DISP) data were obtained in the form of a 4 by 5-inch positive transparency. The film product was digitized at 7-micron resolution that is commensurate with the 150-m spatial resolution of the original product. Both the DISP and Radarsat-1 data were warped to the geolocated SPOT image using a first degree polynomial and tie points selected at locations judged to be stable.

There are numbers of striking differences between the images. The most obvious differences are the seemingly fresh, sinusoidal cracks present in 1963 along the northeastern 'hook' of the ice rise. By 1995 the cracks have evolved into segmented blocks that are being rotated by the shearing flow past the ice rise.

There are also more subtle variations in flow over time and variability from location to location around the ice rise. The DISP image suggests a number of small ice rumples south southwest of the main ice rise (location a in fig. 2). The region downstream of the ice rumples seems to be largely crevasse free. By the mid 1990s, crevasses are clearly evident and surround several of the rumpled areas. Crevasses on the eastern flank of the southern part of the ice rise are nearly unchanged over the same period (b fig. 2). The interior of the ice rise northern embayment, or 'hook', seems relatively undeformed in the 1963 image. The radar image suggests it is cut by long arcuate crevasses formed in response to the shearing flow past the embayment. However, the appearance of the crevasses in the SAR imagery may well

Fig 2. 1963 DISP image portion (120 km across). Solid lines are lineaments based on 1995 SPOT image. Dashed lines are lineaments based on 1997 Radarsat image

be a consequence of the penetration of microwave energy into snow bridges – revealing crevasses undetectable in either the DISP or SPOT data.

Remarkably, a number of objects east of the ice rise are evident between the imagery. These reveal a counterclockwise rotational component to ice flow that becomes more pronounced to the north. Speeds off the southern flank of the ice rise are about 130 m per year (c). Near the right hand portion of the hook speeds drop to about 35-m per year (d) and there is little evidence for motion with the embayment itself. Speeds are about 350 m per year 10 km downstream of the northern nose of the ice stream. Speeds increase 25 % after about 25 km of downstream flow based on the position of the large rifts that form episodically at the northern tip of the ice stream.

Finally, the grounding line on the southwestern flank of the ice rise has advanced outward and upglacier by about 1500 m between 1963 and 1997. This is consistent with ice thickening along this flank of the ice rise and with little ice thickness change along the southeastern flank. Ice thickening may also explain the onset of extensive crevassing along the southwestern flank. There will be more extensive coupling between the ice and the bed as the ice thickens in the ice rumple region. The coupling will lead to increased basal shear stresses which will be manifest as surface crevasses.

SUMMARY

Large portions of this sector of Antarctica are susceptible to dramatic changes in ice flow. Ice streams, large rivers of ice that drain the West Antarctic Ice Sheet into the Ross Ice Shelf, are known to turn 'on and off' on time periods of many 100's of years. This in turn leads to local changes in the grounding line, the location where the terrestrial ice sheet goes afloat. It is believed that rapid changes in ice sheet behavior are in fact due to changes in the internal dynamics of the ice sheet. Rather than external climate forces, changes in glacier physical properties, such as subglacial water flow patterns, are presumed to be the important feedback mechanisms controlling rapid changes in the ice sheet. The structure of Crary Ice Rise eventually responds to inland ice sheet changes by growing or retreating as the upstream ice flux shifts. This may be what we observing today.

The present pattern of thinning along the northeastern margin of the ice shelf and thickening along the southwestern margin may have been repeated in the past [8]. Evidence for this comes from ice thickness patterns far downstream of the ice rise. Here, the ice shelf acts as a 'tape-recorder' preserving remnants of ice thickness patterns of an earlier time. Paired ice thickness hollows and domes similar to the pattern seen today are located about 200 km downstream of the ice rise. Using present day ice velocities, these observations suggest a similar process occurred around the ice rise some 400 years ago. The Corona, SPOT and Radarsat data suggest researchers may now have an opportunity to study a repeat of that same, and perhaps episodic, process.

ACKNOWLEDGMENTS

This work was supported by NASA and under a cooperative agreement with the Canadian Space Agency. G. Hamilton contributed to the data analysis.

REFERENCES

[1] Macdonald, R.A, 1995. Corona: Success for space reconnaissance. A look into the cold war and a revolution in intelligence. Photogramm. Eng. Remote Sens., LXI, p 321-325.

[2] Committee on Environmental and Natural Resources Research, 1997. Our Changing Planet: The FY 1997 U.S. Global Change Research Program.

[3] Bindschadler, R. and P. Vornberger, 1998. Changes in the West Antarctic Ice Sheet since 1963 from Declassified Satellite Photography. Science, vol. 279, p. 689-692.

[4] Paulsen, T. and T. Wilson, 1998. Declassified Intelligence Satellite Photographs (DISP) provide first high-resolution space-borne views of the Transantarctic Mountains in the Antarctic interior. EOS, vol. 79, no. 8,

[5] Jezek, K.C., H.G. Sohn, and K.F. Noltimier, in press. The Radarsat Antarctic Mapping Project. Proceedings IGARSS'98, Seattle, WA.

[6] Jezek, K.C. and 11 others, in press. Snapshots of Antarctica from Radarsat-1. Proceedings IGARSS'98, Seattle, WA.

[7] Bindschadler, R., 1993. Siple Coast Project research of Crary Ice Rise and the mouths of Ice Streams Band C, West Antarctica: review and new perspectives. J. of Glac., vol. 39, no. 133, p. 538-552.

[8] Jezek, K.C., 1984. Recent changes in the dynamical condition of the Ross Ice Shelf, Antarctica. J. Geophys. Res., vol. 89, no. B1, p. 409-416.

[2]Evidence for the Tectonic Segmentation of the Antarctic Peninsula from Integrated ERS-1 SAR Mosaic and Aeromagnetic Anomaly Data

Katy F. Noltimier, Kenneth C. Jezek, Terry J. Wilson, Byrd Polar Research Center, The Ohio State University, 1090 Carmack Road, Columbus, Ohio 43210; tel (614) 292-1107, fax (614) 292-4697; kfn@iceberg.mps.ohio-state.edu
Ash C. Johnson, Geosoft Europe Ltd., 20/21 Market Place, Oxfordshire, United Kingdom; ash@geosofteurope.co.uk

ABSTRACT

The Antarctic Peninsula (AP) is a Mesozoic-Cenozoic Andean-type magmatic arc resulting from subduction of Pacific Ocean lithosphere beneath its western margin. During the past 60 million years discrete segments of the Pacific-Phoenix spreading ridge have successively collided with the western margin of the AP diachronously from south to north in a series of ridge-crest collision episodes. Previous work suggested that the AP (upper plate) was tectonically segmented due to subduction of discrete ridge-crest segments, with segments bounded by the projection of oceanic fracture zones (OFZ). An ERS-1 SAR mosaic was created over the Graham Land-Palmer Land Transition Zone (TZ) and combined with aeromagnetic anomaly and mapped geologic data to study how the process of OFZ subduction modified AP structure. Good correlation of SAR lineament trends and mapped fault trends on Alexander Island provide evidence that some of the SAR lineaments are structurally controlled. Correlation between the SAR and aeromagnetic lineaments suggests both mark crustal structures in the TZ. A model invoking distributed left-lateral fault motion can produce that tight dextral curvature across the TZ and explain the lineament patterns. Correlation between lineament trends and OFZ traces suggests that faulting reflects the response of the AP crust to OFZ subduction.

INTRODUCTION

The S-shaped AP (Fig. 1) is nearly 1500km long extending from the eastern end of Palmer Land northward toward South America. It is made up of a continuous, narrow, and snow covered plateau ranging in height between 2500 and 1500m and is severely dissected by deep coastal glaciers [1]. Physiographically the AP is separated into two sections, Graham Land to the north and Palmer Land to the south (Fig. 1). The zone between Graham Land and Palmer Land was termed the Transition Zone [1], defined where the exposed width of the peninsula dramatically thins, the curvature changes from sinistral to dextral, and there is significant dissection by glaciers.

OBJECTIVES AND METHODS

The primary objectives of this research were to investigate what new information could be obtained from high resolution SAR imagery in order to better understand how the process of OFZ subduction modified the AP structure and to investigate

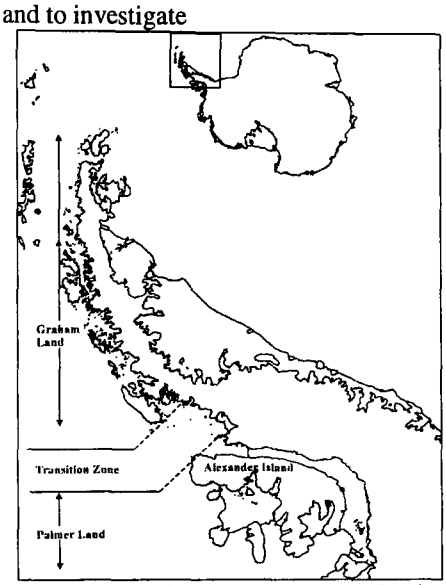

Fig. 1. Geographic location of the Antarctic Peninsula.

geologic and tectonic processes that occurred at the Graham Land-Palmer Land TZ. To test the hypothesis that the unique structure of the TZ formed in response to OFZ subduction, the TZ was examined in detail. SAR lineament trends were compared with detailed aeromagnetic lineament trends and trends in structural geologic data. To model the dominant lineament trends, a Riedel Model for left-lateral faulting was utilized. To explain the lineament patterns and the tight dextral curvature of the AP across the TZ, a model for oroclinal bending [2] was examined.

DETAILED SAR MOSAIC

Because SAR produces high-resolution imagery, it provides the opportunity to focus in more detail on areas of interest relevant to past tectonic events. The detailed SAR mosaic (Fig. 2) provides a comprehensive view of the TZ

[2] Sponsored by NSF Office of Polar Programs

bounded by the Adelaide Fracture Zone (FZ) to the north and the Tula FZ to the south.

There is heavy dissection of glaciers in the TZ. Such glacier swarms are first indicators that major faulting may have occurred. The Adelaide FZ crosses onto the AP in the vicinity of Neny Glacier. Wyeth [1] noted that the Neny-Gibbs glacial trough marks a fault line based on geologic evidence of NW trending faults in the vicinity of Kenyon Peninsula. If this is true, then the Neny-Gibbs glacial trough may mark the onshore extension of the Adelaide FZ.

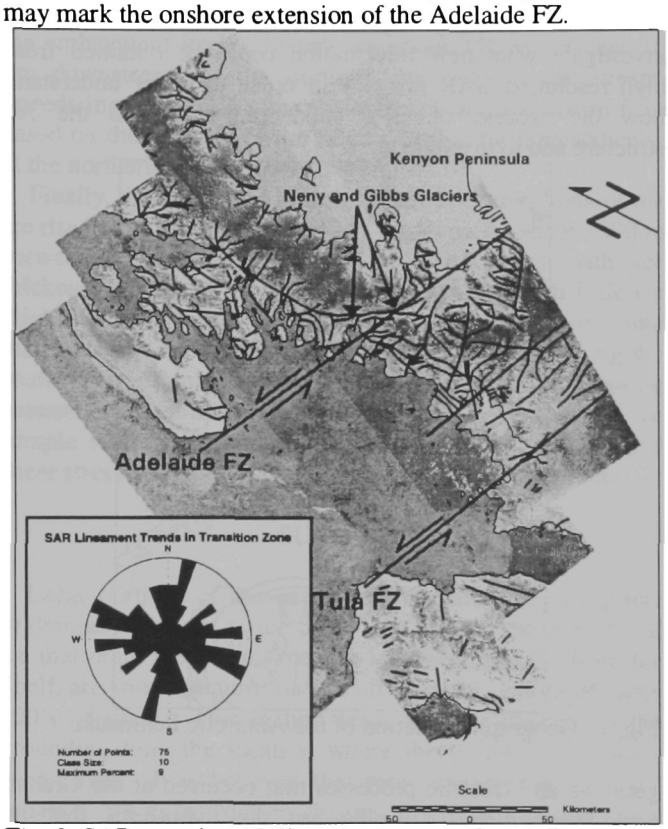

Fig. 2. SAR mosaic with lineament map and rose diagram.

SAR LINEAMENTS AND TRENDS IN STRUCTURAL GEOLOGIC DATA

A lineament map was derived from glacial drainage patterns visible on the SAR mosaic (Fig. 2). A rose diagram reveals three main trends in the SAR lineaments (Fig 2, inset) To determine whether linear features visible on the SAR mosaic correlate with structural bedrock features, the SAR lineament trends were compared with trends in structural geologic data.

Fault, dyke, bedding, and rock cleavage trends within the TZ were measured directly from the BAS Geological Maps and compiled into rose diagrams (Fig. 3). Due to the limited number of mapped faults (four), fault trends are inconclusive. However, dyke trends show a prominent N-NW (330°-360°) clustering as do the bedding (350°-360°) and rock cleavage trends (330°-350°). The N-NW trends correspond with one cluster of SAR lineament trends. There is a lesser E-W (270°-290°) clustering of dyke trends.

Due to the lack of mapped faults in the TZ, rose diagrams were constructed to compare mapped fault trends measured on Alexander Island with SAR lineament trends. Alexander Island is an area where detailed ground-derived information is readily available, making it an ideal location for a comparative study. Mapped fault trends (Fig. 4, left) show a prominent 350°-360° trend with a lesser 290°-300° trend in the NW quadrant. SAR lineament trends (Fig. 4, right) agree well with the mapped N-S fault trends providing evidence that SAR lineaments mark faults in this region.

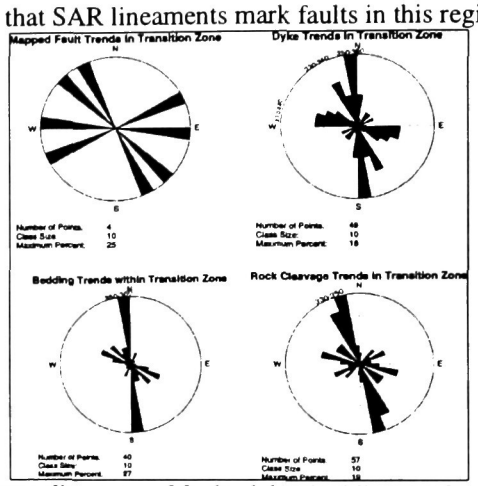

Fig. 3. Rose diagrams of fault, dyke, bedding, and rock cleavage trends within the TZ.

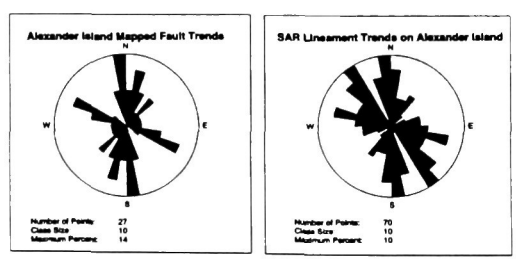

Fig. 4. Rose diagrams of mapped fault and SAR lineament trends on Alexander Island.

AEROMAGNETIC LINEAMENTS

The aeromagnetic anomaly map and aeromagnetic lineaments (Fig. 5) were derived from a detailed (3km grid spacing) aeromagnetic survey of the TZ [3]. There is an over all NW-SE trend in the magnetic fabric as evident in an elongate positive anomaly extending into Marguerite Bay (Fig.5A) trending NW-SE. Johnson and Swain conclude that: (1) the prominent NW-SE (315°) trend of the magnetic fabric supports a link between the magnetic lineations and extrapolated OFZ (Fig. 5C, D). (2) The apparent left-lateral offset of the western side of the Pacific Margin Anomaly (PMA) suggests the OFZ are faults with a component of left-lateral strike-slip motion. (3) The area of subdued anomalies west of the PMA is a down-faulted block (Fig. 5C) believed to be the result of ridge-crest arrival at the trench.

A rose diagram of the onshore aeromagnetic lineament trends (Fig. 5, inset) shows a prominent 300°-320° trend corresponding well with the aeromagnetic observations.

COMBINED LINEAMENT MAPS

The correlation between the two types of lineaments strongly suggests that both SAR and aeromagnetic lineaments mark crustal structures. Rose diagrams of the SAR and onshore aeromagnetic lineament trends were intercompared with a Riedel Model for left-lateral faulting with a main shear trend of 305° to demonstrate more clearly the angular relationships (Fig. 6). The main shear trend of 305° is a best-

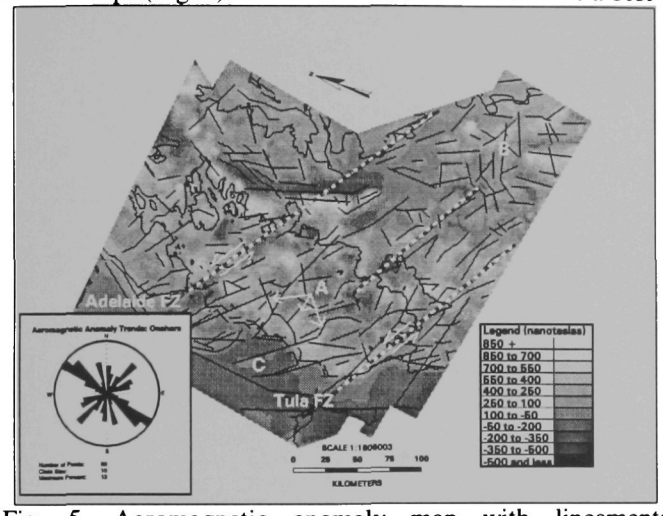

Fig. 5. Aeromagnetic anomaly map with lineaments (modified from [3]).

fit estimate between the prominent SAR and aeromagnetic lineament trends. The good angular match between the Riedel Model and the SAR lineament trends (Fig. 6) suggests a viable model for the lineament patterns in the TZ invoking left-lateral fault motion. The onshore aeromagnetic lineament trends (Fig. 6) also have a reasonably good angular relationship with the Riedel Model. The correlation of the SAR and aeromagnetic lineament trends with the Riedel Model support a model for left-lateral faulting in the TZ in response to subduction of OFZ.

STRIKE-SLIP BENDING MODEL

Cunningham [2] proposed a left-lateral strike-slip model to explain the curvature of the southernmost South America. This model is based on the existence of regional strike-slip faulting, rotation and translation of southernmost Andes crustal blocks, and relative plate motions through time. He integrated field data and existing paleomagnetic data with the existence of widespread lineaments that were statistically consistent in orientation with the Riedel Model for left-lateral faulting. A similar model could explain the tight dextral curvature of the AP in the TZ. The SAR and aeromagnetic lineament patterns are compatible with left-lateral fault motion associated with an extensional environment. Distributed left-lateral faulting could offset the AP axis and produce a dextral curvature across the TZ by crustal block displacement (Fig. 7).

CONCLUSIONS

The strongly dissected nature of the TZ, defined by SAR lineaments, led to the hypothesis that the exposed portion of at least some SAR lineaments represent faults from the good correlation between mapped fault trends on Alexander Island and SAR lineament trends. The hypothesis that SAR lineaments mark crustal structures is also confirmed by correlation between the SAR and aeromagnetic lineament trends. Based on previous interpretations for the TZ, a

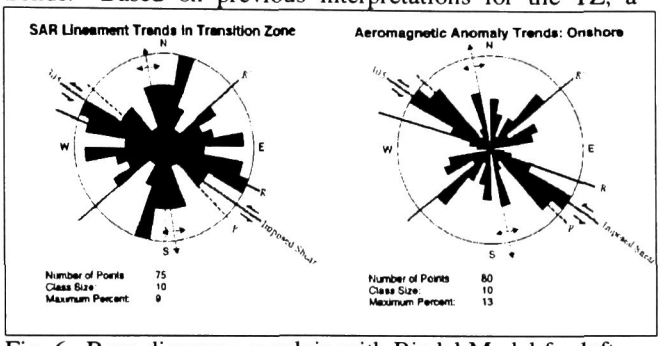

Fig. 6. Rose diagrams overlain with Riedel Model for left lateral faulting.

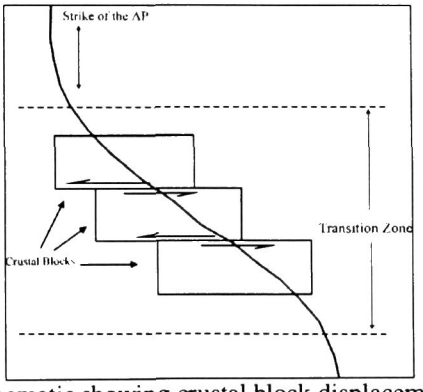

Fig. 7. Schematic showing crustal block displacement westward producing apparent offset of AP and dextral curvature across the TZ.

hypothesis that SAR lineaments in the TZ record left-lateral faulting was developed. The good angular relation between lineament trends is compatible with left-lateral the Riedel Model for left-lateral faulting and SAR and aeromagnetic strike-slip shearing across the TZ. These relations are in agreement with previous evidence that the apparent left-lateral offset of the PMA was the result of left-lateral strike-slip motion. Correlation in the dominant trends of the SAR and aeromagnetic lineament trends (290°-330°) with OFZ trends (315°) suggests that left-lateral faulting was in response to OFZ subduction. A model for distributed left-lateral faulting was presented as a mechanism for the block displacement.

REFERENCES

[1] Wyeth, R. B., 1977. "The Physiography and Significance of the Transition Zone between Graham Land and Palmer Land". British Antarctic Survey Bulletin, No. 46, 39-58.

[2] Cunningham, W. D., 1993. "Strike-slip Faults in the Southernmost Andes and the Development of the Patagonian Orocline". Tectonic, Vol. 12, No. 1, 169-186.

[3] Johnson, A. C., and C. J. Swain, 1995. :Further Evidence of Fracture-Zone Induced Tectonic Segmentation of the Antarctic Peninsula from Detailed Aeromagnetic Anomalies". Geophysical Research Letters, Vol. 22, No. 14, 1917-1920.